HHS Public Access

Author manuscript

Cell Rep. Author manuscript; available in PMC 2016 March 24.

Published in final edited form as:

Cell Rep. 2015 March 24; 10(11): 1899–1912. doi:10.1016/j.celrep.2015.02.041.

Mouse low-grade gliomas contain cancer stem cells with unique molecular and functional properties

Yi-Hsien Chen[1], **Lucy D'Agostino McGowan**[1], **Patrick J. Cimino**[2], **Sonika Dahiya**[2], **Jeffrey R. Leonard**[3], **Da Yong Lee**[1], and **David H. Gutmann**[1]

[1]Department of Neurology, Washington University School of Medicine, St. Louis MO 63110, USA

[2]Department of Pathology, Washington University School of Medicine, St. Louis MO 63110, USA

[3]Department of Neurosurgery, Washington University School of Medicine, St. Louis MO 63110, USA

Summary

The availability of adult malignant glioma stem cells (GSCs) has provided unprecedented opportunities to identify the mechanisms underlying treatment resistance. Unfortunately, there is a lack of comparable reagents for the study of pediatric low-grade glioma (LGG). Leveraging a neurofibromatosis-1 (*Nf1*) genetically-engineered mouse LGG model, we report the isolation of $CD133^+$ multi-potent low-grade glioma stem cells (LG-GSCs), which generate glioma-like lesions histologically similar to the parent tumor following injection into immunocompetent hosts. In addition, we demonstrate that these LG-GSCs harbor selective resistance to currently-employed conventional and biologically-targeted anti-cancer agents, which reflect the acquisition of new targetable signaling pathway abnormalities. Using transcriptomal analysis to identify additional molecular properties, we discovered that mouse and human LG-GSCs harbor high levels of Abcg1 expression critical for protecting against endoplasmic reticulum (ER) stress-induced mouse LG-GSC apoptosis. Collectively, these findings establish that LGG cancer stem cells have unique molecular and functional properties relevant to brain cancer treatment.

Keywords

astrocytoma; neurosphere; tumor-initiating cell; neurofibromatosis; mTOR; ABCG1

Address correspondence to: David H. Gutmann, MD, PhD, Department of Neurology, Washington University School of Medicine, Box 8111, 660 S. Euclid Avenue, St. Louis MO 63110. 314-362-7379 (Phone); 314-362-2388 (FAX); gutmannd@neuro.wustl.edu.

Author Contributions

DHG supervised the research. DHG, Y-HC conceived and designed the experiments. Y-HC performed the experiments and analyzed the data. LDM analyzed the microarray data. PJC and SD provided human specimens and helpful discussions. Human glioma stem cells were provided by JRL. DYL initiated the project and generated initial optic glioma stem cells for the microarray analysis. Y-HC, DHG contributed materials/analysis tools. Y-HC, DHG wrote the manuscript. All authors edited and approved the manuscript.

Introduction

Numerous cancers are maintained by small populations of cells with stem cell-like properties (Hope et al., 2004; Kim et al., 2005; Ricci-Vitiani et al., 2007), including those of the nervous system (Singh et al., 2004). These stem cells have the capacity for self-perpetuation as well as to generate mature cells of specific tissue lineages (Bonnet and Dick, 1997; Kim et al., 2005; Singh et al., 2003; Vermeulen et al., 2008), and in this respect, represent good candidates for therapeutic intervention. The importance of this population to brain tumor biology is underscored by the demonstration that cancer stem cells (CSCs) generate tumors following injection into immunocompromised mice with similar histologic and growth properties to the parental tumor (Galli et al., 2004; Singh et al., 2004; Taylor et al., 2005). In addition, these CSCs harbor unique responses to conventional therapeutic agents (Beier et al., 2011; Sakariassen et al., 2007), which have broad implications for the design of treatments aimed at eliminating the very cells that maintain and recapitulate the tumor. As such, malignant glioma regrowth following alkylating agent therapy (temozolomide) in mice is due to the relative resistance of CSCs to this agent (Chen et al., 2012). Moreover, many of the markers expressed by CSCs also serve as independent predictors of survival in patients with these malignancies (Hale et al., 2014; Lathia et al., 2014; Pietras et al., 2014).

In contrast, the study of CSCs in low-grade gliomas (LGGs) has been hampered by their low clonogenic frequencies (Singh et al., 2003), technical difficulties inherent in maintaining these cells in culture (Raabe et al., 2011), and the inability to generate tumors following xenografting. Complicating the issue in the context of neurofibromatosis type 1 (NF1), the most common inherited disorder in which affected children develop LGG, is the limited availability of tumor specimens, exquisite brain region constraints important for tumor initiation and growth (Lee da et al., 2012), and dependence on *NF1*+/− non-neoplastic immune system-like cells (microglia) for glioma formation and maintenance (Daginakatte and Gutmann, 2007; Pong et al., 2013). In this cancer predisposition syndrome, 15–20% of children with NF1 develop World Health Organization (WHO) grade I astrocytomas (low-grade gliomas) involving the optic nerve and chiasm, and less commonly, the brainstem (Guillamo et al., 2003). These human tumors have low proliferative indices (<1%), increased microglia infiltration, and pleiomorphic neoplastic cells with nuclear atypia (Louis et al., 2007).

To identify and characterize LG-GSCs, we leveraged a well-characterized murine model of NF1-associated low-grade optic glioma (Bajenaru et al., 2003) in which *Nf1*+/− mice undergo somatic *Nf1* gene inactivation in neuroglial progenitor cells (*Nf1*+/−^{GFAP}CKO mice). Nearly 100% of *Nf1*+/−^{GFAP}CKO mice develop low-grade gliomas of the optic nerves and chiasm. Similar to their human counterparts, these tumors likewise have low proliferative indices (<1%), microglial infiltration, and pleiomorphic neoplastic cells with nuclear atypia (Bajenaru et al., 2003; Hegedus et al., 2009; Kim et al., 2010). Using this platform, we isolated CD133^{+} cells from tumor-bearing, but not normal, mice that were capable of long-term passage, self-renewal, and multi-lineage differentiation as well as the ability to form glioma-like lesions following transplantation into naïve *Nf1*+/− immunocompetent animals. Relative to their non-neoplastic *Nf1*-deficient neural stem cell

counterparts, these low-grade optic glioma stem cells (o-GSCs) exhibited reduced sensitivity to some conventional and biologically-targeted agents, which reflected the acquisition of targetable escape mechanisms. Transcriptomal analyses revealed that o-GSCs express Abcg1 and Lgr5, which were also found in human low-grade GSCs. Moreover, we demonstrate that Abcg1 was critical for maintaining mouse optic GSC survival through suppression of ER stress. Collectively, this study establishes the existence of a population of CSCs in mouse low-grade glioma with unique functional and molecular properties.

Results

Nf1+/–^{GFAP}CKO mouse optic gliomas contain CD133^{+} stem cells

To determine whether CSCs could be generated from low-grade glioma-bearing mice, single cells were dissociated from the optic nerves/chiasm of *Nf1*$^{flox/flox}$ (wild-type), *Nf1*+/−, and *Nf1*+/−^{GFAP}CKO mice at 3 months of age, and maintained in defined media. After one week culture, neurospheres emerged from *Nf1*+/−^{GFAP}CKO mouse optic nerve cultures (Figure 1A, B). The frequency of this stem cell population in the murine optic gliomas ranged from 0.06% to 0.28% (0.15 +/− 0.11%; n=3), determined using a primary sphere formation assay (Figure 1A). In contrast, cells from *Nf1*$^{flox/flox}$ (WT) and *Nf1*+/− mice took nearly 3 weeks to form smaller clusters, which could not be maintained by serial passaging due to loss of proliferation and self-renewal ability.

Since these mouse *Nf1* optic gliomas (Lee da et al., 2012) as well as some human optic gliomas (Tchoghandjian et al., 2009) likely arise from third ventricular zone (TVZ) neuroglial progenitors, *Nf1*-deficient TVZ neural stem cells (NSCs) were employed as non-neoplastic reference cells (Figure 1C). Both *Nf1*-deficient TVZ NSCs and glioma neurospheres expressed Nestin and Sox2 (Figure 1D) as well as BLBP and Olig2 (Figure S1A, B), but were negative for neurofibromin (Figure 1C) and GFAP expression (Figure S1A). However, only optic GSCs (o-GSCs) expressed CD133 (Figure 1D, E), similar to human PA spheres (Figure S1C). In addition, other GSC markers identified in glioblastoma GSCs (Lathia et al., 2010; Son et al., 2009; Tchoghandjian et al., 2010), including A2B5, CD15 and CD49f, were expressed in o-GSCs, but not in *Nf1*−/− TVZ NSCs (Figure 1D, E).

o-GSCs could be stably maintained for >30 passages without significant changes in their growth rates (Figure S1D). Relative to their non-neoplastic counterparts, o-GSCs had higher frequencies of secondary neurosphere formation (Figure S1E), increased proliferation (Figure 1F and G), decreased cell death (Figure 1H and I), and increased glial differentiation (Figure 1J). Together, these findings establish the presence of *Nf1*-deficient cells with stem cell properties in these low-grade mouse gliomas.

o-GSCs induce glioma-like lesions *in vivo*

To determine whether o-GSCs generate tumors *in vivo*, we transplanted 500,000 mCherry-expressing o-GSCs into the brainstems of 3-week-old *Nf1*+/− mice. *Nf1*+/− mice were chosen to provide a more faithful genetic background, since these tumors arise in patients with a germline *NF1* gene mutation. Brainstem injections were performed, as optic nerve injections are not technically possible, and 15–20% of NF1-associated LGGs arise in the

brainstem (Guillamo et al., 2003). Within six months, all mice transplanted with o-GSCs (n=11 mice) harbored areas of increased cellularity consistent with glioma-like lesions, including abnormal cell clusters (H&E), strong GFAP immunostaining with elongated cytoplasmic processes (Figure S2A), and increased microglial ($Iba1^+$ cells) infiltration relative to the uninjected contralateral sides (Figure 2A, B). Similar to optic gliomas arising in *Nf1*+/−^{GFAP}CKO mice, these ectopic lesions had low proliferative indices (%$Ki67^+$ cells) and increased percentages of $Olig2^+$ and $Iba1^+$ cells (Figure 2B). Consistent with the conclusion that these glioma-like lesions arose from the injected o-GSCs, we found that 66% of the $GFAP^+$ cells, 62% of the $Olig2^+$ cells, and the majority of the $Ki67^+$ (72%) were positive for mCherry expression (Figure 2C). In contrast to o-GSCs, *Nf1*+/− mice (n=4) transplanted with *Nf1*−/− TVZ NSCs did not form glioma-like lesions 6 months post-injection. Unlike the glioma-like lesions generated following o-GSC injection, there was only a modest cell accumulation (H&E) and less robust GFAP immunostaining, but no change in the percentages of $Iba1^+$ and $Olig2^+$ cells, and nearly no proliferating ($Ki67^+$) cells at the injection sites (Figure S2B, C). Importantly, the vast majority of the $GFAP^+$ cells were mCherry-negative (Figure S2D) with stellate morphologies (Figure S2B, inset), indicating that they were likely host-derived reactive astrocytes.

To determine whether the *Nf1*+/− local microenvironment was important for glioma formation, o-GSCs were injected into the brainstems of immunocompromised athymic mice. In striking contrast to the glioma-like lesions generated following o-GSC injection into *Nf1*+/− mice, immunocompromised mice transplanted with o-GSCs did not form gliomas 6 months post-injection. In total, while 3 of 5 mice showed hypercellular lesions with modest GFAP immunostaining and an increased percentage of $Olig2^+$ cells, no changes in the percentages of $Iba1^+$ and $Ki67^+$ cells were observed (Figure 3A, B). Despite the absence of a detectable glioma-like lesion in these mice, there was mCherry expression in the majority of Ki67-, GFAP- and Olig2-immunoreactive cells at the injection sites (Figure 3C). Similarly, there were greater numbers of $Iba1^+$ and $Ki67^+$ cells at these injection sites (Figure S3); however, these increases were ~2- and 3-fold lower than observed in *Nf1*+/− mice, respectively. Together, the development of glioma-like lesions following o-GSC transplantation demonstrates the gliomagenic nature of these low-grade glioma stem cells in concert with the need for a supportive microenvironment.

o-GSCs exhibit selective resistance to anti-cancer treatments

Emerging evidence supports the concept that high-grade CSCs may be resistant to therapeutic agents and radiotherapy used to treat patients with these brain tumors (Bao et al., 2006; Chen et al., 2012; Liu et al., 2006). To explore the possibility that o-GSCs might be less sensitive to conventional (Pace et al., 2003; Packer et al., 1993) or new biologically-targeted therapies [rapamycin analogs, NCT01734512 and NCT01158651; MEK inhibitors, NCT01885195], we exposed *Nf1*-deficient TVZ NSCs and o-GSCs to vincristine, temozolomide, carboplatin, rapamycin (Rap), and the PD0325901 (PD901) MEK inhibitor. While o-GSCs and *Nf1*−/− TVZ NSCs were equally sensitive to temozolomide (Figure 4A) and vincristine (Figure 4B), o-GSCs were more resistant to carboplatin (5-fold increased ED50; Figure 4C), rapamycin (6-fold increased ED50; Figure 4D), and PD901 (3-fold increased ED50; Figure 4E) treatments.

Whereas rapamycin inhibited mTOR activity in a dose-dependent fashion, as measured by S6 phosphorylation (Figure S4), the resistance to rapamycin was the consequence of increased mTOR activation in o-GSCs relative to *Nf1*−/− TVZ NSCs (1.5- and 1.7-fold increases S6 $Ser^{240/244}$ and $Ser^{235/236}$ phosphorylation, respectively; Figure 5A). Previous studies in other cell types have demonstrated that mTOR can be additionally activated by loss of tuberous sclerosis complex (TSC) function (Kwiatkowski et al., 2002; Ma et al., 2005; Manning et al., 2002) or p90-RSK-mediated phosphorylation (Carriere et al., 2008). While we observed no change in total tuberin expression, there was increased hamartin expression in both *Nf1*−/− TVZ NSCs and o-GSCs, and a decrease in phosphorylation-mediated tuberin inactivation (Ser^{939} and Thr^{1462}), excluding tuberin/hamartin-mediated mTOR activation as the mechanism underlying the increased mTOR activity in o-GSCs (Figure S5A). In contrast, o-GSCs exhibited increased p90-RSK activation (3-fold increase in p90-RSK-Thr^{573} phosphorylation; Figure 5B). To demonstrate that this acquired p90-RSK hyper-phosphorylation was responsible for the increased mTOR activation in o-GSCs, o-GSCs were treated with rapamycin and SL0101 (p90-RSK inhibitor). Consistent with a model in which p90-RSK further activates mTOR signaling in o-GSCs, SL0101 treatment ameliorated the observed S6 hyper-phosphorylation and relative resistance to rapamycin growth inhibition (Figure 5C).

While the reduced sensitivity to rapamycin resulted from p90-RSK-mediated mTOR hyperactivation, o-GSC relative resistance to PD901 treatment was not due to differences in basal ERK activity (Figure S5B). Moreover, PD901 did not inhibit ERK-Thr^{202}/Tyr^{204} phosphorylation as a result of aberrant MEK activation (phospho-MEK-$Ser^{217/221}$; Figure 5D). In *KRAS* mutant human tumors, reactivation of CRAF creates a MEK-CRAF complex, which increases MEK/ERK phosphorylation after PD901 treatment (Lito et al., 2014). Consistent with this mechanism, PD901 treatment induced MEK binding to CRAF, and resulted in increased CRAF activity (CRAF Ser^{338} phosphorylation) only in o-GSCs (Figure 5E). To determine whether this aberrant activation of CRAF was responsible for MEK inhibitor resistance, o-GSCs were treated with trametinib, a MEK inhibitor that blocks the association between MEK and CRAF (Lito et al., 2014). Trametinib reduced o-GSC MEK/CRAF binding (Figure 5F), ERK/MEK hyperactivation (Figure 5G), and o-GSC growth (Figure 5H). Together, these findings reveal new mechanisms for o-GSC chemoresistance, which can be targeted to inhibit the growth of these CSCs.

o-GSCs exhibit increased Abcg1 expression

In addition to the acquiring escape mechanisms to biologically-targeted therapies, we also sought to identify potential molecular differences between o-GSCs and their non-neoplastic *Nf1*-deficient NSC counterparts. Microarray gene expression analysis revealed 59 genes with >5-fold increased expression in o-GSCs relative to *Nf1*−/− TVZ NSCs (Figure 6A; Table S1), whereas 87 genes were decreased by at least 5-fold in o-GSCs (Table S2). We next prioritized candidate genes based on their function, including transcription factors, growth regulators, cell surface markers, and stem cell proteins. The majority of candidate transcripts showed subtle increases in expression (1.3 to 2-fold up-regulation) upon real-time quantitative PCR (qPCR; data not shown) validation. However, two transcripts, *Abcg1* and *Lgr5*, were overexpressed >3-fold in o-GSCs by qPCR and Western blotting relative to

Nf1-deficient or *Nf1*+/− (Figures 6B–C, S6A–C) NSCs from three brain germinal regions (dentate gyrus, subventricular zone, third ventricle). Consistent with these *in vitro* results, ~20% of the cells in the intact parental *Nf1*+/−^{GFAP} CKO mouse optic glioma were Abcg1- or Lgr5-immunoreactive *in vivo* (Figure 6D). In addition, ABCG1 and LGR5 were also expressed in human pilocytic astrocytomas (PA) spheres generated from two fresh surgical specimens (Figure 6E). These PA spheres could not be maintained beyond two passages, limiting the evaluation of ABCG1 and LGR5 in human LG-GSCs. It is worth noting that no changes in the expression of other ABC family genes were identified (Figure S6D), including ABCG2, which defines the GSC side population (Bleau et al., 2009). As such, ABCG2 expression was detected in human GBM spheres, but not in either o-GSCs or human PA spheres (Figure S6E).

Abcg1 expression is critical for enhanced o-GSC survival

Whereas several studies have shown that LGR5 is important for glioblastoma CSC function and patient survival (Nakata et al., 2013; Parry and Engh, 2014; Wang et al., 2014), the role of ABCG1 in glioma pathogenesis is unknown. ABCG1 is a member of a large superfamily of membrane-bound ATP-binding cassette (ABC)-containing proteins important for cellular transport (Tarling and Edwards, 2011; Wang et al., 2004), where it directs lipid transport (Kennedy et al., 2005; Klucken et al., 2000). Given the putative role of Abcg1 as a potential unique glioma stem cell marker, we initially investigated ABCG1 expression in human NF1-associated PA specimens. ABCG1 immunoreactivity was observed in both human NF1-associated optic pathway (n=3) and non-optic pathway gliomas (n=3) (Figure 7A), representing 23–35% (27 +/− 6%) of the total tumor area similar to that observed in the murine *Nf1* optic gliomas.

Next, we employed shRNA knockdown to define the functional relevance of ABCG1 to o-GSC biology. First, knockdown of *Abcg1* expression using two different lentiviral-mediated shRNA constructs (Figure 7B; 50–60% protein reduction) reduced o-GSC growth and self-renewal by 40–46% (Figure 7C) and 76–78% (Figure 7D), respectively. This decrease in cell number was not the result of reduced proliferation (Figure 7E), but rather reflected a 2-fold increase in apoptosis (Figure 7F).

Second, to determine whether caspase activation (cleavage) was induced in Abcg1 knockdown-induced apoptosis, caspase pathway activation in o-GSCs following shAbcg1 silencing was examined. Cleavage of one initiator caspase (caspase-12, but not caspase-9) as well as the caspase-6, caspase-3, and poly (ADP-ribose) polymerase (PARP) downstream effectors, was observed in o-GSCs after Abcg1 shRNA-mediated knockdown (Figure 7G–H).

Finally, to determine whether ER stress was responsible for Abcg1 knockdown-induced cell death, the expression of BiP and CHOP, two markers of ER stress (Liu et al., 1997; Zinszner et al., 1998) were examined. Abcg1 knockdown increased BiP and CHOP expression by 2 to 2.5-fold and 4.5 to 7-fold, respectively, relative to controls (Figure 7I). Tunicamycin was included as a positive control for ER stress induction. Moreover, BiP, CHOP, cleaved caspase-3, and cleaved PARP expression in Abcg1 knockdown o-GSCs were reduced to control levels (Figure 7J) following 4-phenyl butyric acid (PBA) treatment, a treatment

capable of blocking ER stress (Erbay et al., 2009; Ozcan et al., 2006). Together, these results demonstrate that Abcg1 provides a survival advantage to o-GSCs by suppressing ER stress induction (Figure 7K).

Discussion

The challenges to studying low-grade GSCs in humans partly reflect their low clonogenic frequencies, estimated at 0.3–1.5%, relative to high-grade brain tumors (8–25%) grown under the same conditions (Singh et al., 2004). In addition, the failure to generate tumors following human low-grade GSC implantation into immunocompromised mice may reflect the exquisite brain region specificity and need for a permissive tumor microenvironment. In this regard, NSCs from different CNS regions exhibit unique molecular signatures (Horiguchi et al., 2004; Kim et al., 2006) and respond differentially to specific cancer-causing genetic changes (Kaul et al., 2012; Lee da et al., 2012), including *Nf1* gene inactivation (Lee da et al., 2010). Moreover, non-neoplastic stromal cells (e.g., microglia) are important for both mouse *Nf1* optic glioma development (Pong et al., 2013) and maintenance (Daginakatte and Gutmann, 2007), such that disruption of their function delays optic gliomagenesis and reduces tumor proliferation.

Based on these considerations, we leveraged a well characterized murine model of NF1 low-grade glioma, in which tumors arise in the optic nerve. Using this platform, we identified a population of cells with neural stem cell properties that were additionally capable of forming glioma-like gliomas following transplantation into *Nf1*+/− mice. Similar to human low-grade GSCs, the clonogenic frequency of o-GSCs in these tumors was less than 1%. In addition, as observed in human GSCs, o-GSCs expressed the CD133, A2B5, CD15, and CD49f stem cell markers.

The deployment of this murine low-grade glioma system reduced the time from tumor removal to *in vitro* expansion, thus facilitating a detailed examination of the unique molecular and cellular properties of these low-grade GSCs. First, we demonstrate that o-GSCs form glioma-like lesions following injection into the brainstems of *Nf1*+/− mice, a region where gliomas form in children with NF1 who harbor a germline *NF1* gene mutation. In striking contrast, *Nf1*-deficient TVZ NSCs did not generate gliomas following transplantation, revealing cellular properties unique to the o-GSCs not shared with their non-neoplastic *Nf1*−/− counterparts. The importance of the *Nf1*+/− supportive microenvironment was further underscored by a failure to generate glioma-like lesions following o-GSC injection into the brainstems of athymic mice.

Second, o-GSCs exhibited a relative selective resistance to some agents currently used to treat these tumors in children with NF1. Specifically, carboplatin is often the first-line chemotherapy employed for children with NF1-optic glioma (Mahoney et al., 2000; Packer et al., 1997). The relative resistance to this agent may explain why some optic gliomas continue to grow and require alternative second-line therapies. Similarly, recent clinical trials have employed rapamycin analogs based on preclinical evidence demonstrating that rapamycin suppresses murine *Nf1* optic glioma proliferation (Hegedus et al., 2008). In these murine proof-of-principle studies, 5 mg/kg/day rapamycin treatment did not produce a

durable response, with tumor regrowth following the discontinuation of drug, whereas 20 mg/kg/day rapamycin was required for continued optic glioma growth suppression following drug withdrawal. These preclinical observations are consistent with the reduced rapamycin sensitivity observed in o-GSCs, and suggest that durable responses may require higher mTOR inhibitor drug dosing. In this regard, the increased mTOR activation in o-GSCs was mediated by acquired p90-RSK hyperactivation, such that the relative rapamycin resistance could be ameliorated following combined p90-RSK and mTOR inhibition.

Previous work has shown that *NF1*-deficient GBM cells have variable degrees of MEK inhibitor sensitivity (See et al., 2012). This relative MEK inhibitor sensitivity was also observed in o-GSCs, which results from MEK/CRAF binding and CRAF activation such that treatment with a MEK inhibitor (trametinib) that additionally promotes the dissociation of MEK from CRAF effectively blocked o-GSC growth. Current preclinical studies are planned to compare PD901 to trametinib therapy for *Nf1* murine optic glioma.

Third, we identified ABCG1 and LGR5 as GSC markers. While LGR5 has been previously shown to control glioma proliferation (Parry and Engh, 2014; Wang et al., 2014), little is known about ABCG1 function in cancer. Like ABCG2, ABCG1 is a member of a large superfamily of membrane-bound ATP-binding cassette (ABC)-containing proteins important for cellular transport (Tarling and Edwards, 2011; Wang et al., 2004), where it mainly directs lipid transport (Kennedy et al., 2005; Klucken et al., 2000). However, ABCG2 was not highly expressed in o-GSCs as it is in high-grade GSCs (Figure S4E), consistent with an absence of a side population following Hoechst 33342 flow cytometry (data not shown). While the classification of glioma stem cells based on ABCG2 expression is currently controversial (Golebiewska et al., 2013), the isolation of human low-grade GSCs using Hoechst 33342-mediated flow cytometry would likely be unsuccessful.

Previous studies have suggested that downregulation of ABCG1 can induce apoptosis in other cell types (Tarling et al., 2010; Yvan-Charvet et al., 2010), perhaps in response to intracellular lipid accumulation and subsequent endoplasmic reticulum (ER) stress (Tarling and Edwards, 2011; Wojcik et al., 2008; Xue et al., 2013; Yvan-Charvet et al., 2007). In this report, we demonstrate that Abcg1 knockdown increased ER stress protein expression and apoptosis, which could be rescued by PBA treatment. The adaption to the ER stress is one critical mechanism for promoting tumor cell growth and survival. In this regard, tumor cells use adaptive pathways to circumvent the cellular stress conditions associated with hypoxia, low glucose levels, or chemotherapeutic drug exposure (Li and Lee, 2006; Luo and Lee, 2013). As such, strategies aimed at blocking these adaptations may improve treatment efficacy (Booth et al., 2014; Cho et al., 2014; Ciechomska et al., 2013; Johnson et al., 2014; Liu et al., 2013; Suzuki et al., 2013). While the precise mechanism responsible for ABCG1-mediated suppression of ER stress remains to be elucidated, its potential importance to glioma biology is underscored by preliminary studies demonstrating that high *ABCG1* expression correlated with shorter overall survival in patients with glioblastoma of the mesenchymal subtype (Jingqin Luo, unpublished results). Further investigation of ABCG1-mediated ER stress suppression in cancer could lead to the development of new therapeutic approaches targeted against gliomas characterized by increased Abcg1 expression.

In summary, we have successfully leveraged *Nf1* GEM strains to identify and characterize a previously difficult-to-study population of CSCs from low-grade glioma. This strategy not only revealed differential drug sensitivities relevant to future therapeutic targeting efforts, but also highlighted the critical role of Abcg1 for o-GSC survival through the suppression of ER stress.

Experimental Procedures

Mice

All strains were generated (Supplemental Experimental Procedures), maintained on a C57BL/6 background, and used in accordance with an approved Animal Studies protocol at Washington University. Athymic (B6.Cg/NTac-*Foxn1nu* NE10) mice were purchased from Taconic Laboratories.

Primary NSC isolation and culture

Optic chiasm was microdissected from 3-month-old $Nf1^{flox/flox}$, *Nf1*+/− and $Nf1+/-^{GFAP}$CKO mice to generate primary optic nerve neurospheres. TVZ NSCs were established from the third ventricle of 3-month-old $Nf1^{flox/flox}$ and *Nf1*+/− mice. NSC cultures and proliferation assays were performed as previously described (Lee da et al., 2010). Wild-type and *Nf1*−/− NSCs were generated from $Nf1^{flox/flox}$ mouse brains following infection with Ad5-LacZ and Ad5-Cre adenovirus (University of Iowa Gene Transfer Core, Iowa City, IA), respectively. Loss of neurofibromin protein was confirmed by Western blotting. All *in vitro* experiments were performed at least three times using primary NSC generated using mice from different litters, and independently transduced with the respective constructs (Table S3).

Human tumor spheres

Human PA and GBM specimens were obtained from the Children's Discovery Institute Tumor Bank at the Washington University School of Medicine, and used under an approved Human Studies Protocol. Fresh human tumor specimens were minced into small pieces and dissociated in accutase at 37°C. Single cells were obtained and cultured in tumor sphere media (TSM) containing Neurobasal-A media supplemented with Glutamax, EGF (20ng/ml), FGF (20ng/ml), leukemia inhibitory factor (20ng/ml), N2, B-27, and heparin (20ng/ml). Additional human PA and GBM paraffin sections were used from available clinical materials under an approved Human Studies Protocol.

Multi-lineage differentiation

Neurospheres were trypsinized and plated onto 24 well plates coated with poly-D-lysine (50 μg/ml) and fibronectin (10 μg/ml) in defined NSC medium containing N2, B27 and 1% FBS without growth factors. After 6 days, the cells were fixed with 4% paraformaldehyde and stained with antibodies against Tuj-1 (neuron), O4 (oligodendrocyte) and GFAP (astrocyte). The primary antibodies used are listed in Table S4.

Lentivirus infections

Abcg1 shRNA or control shGFP-containing pLKO.1 plasmid was co-transfected with pMDLg/pRRE, pRSV-REV and pCMV-VSV-G into HEK293T cells using the FuGENEHD transfection reagent (Roche). o-GSCs were dissociated into single cells by trypsin and transduced with viral supernatants from HEK293T cells. The knockdown efficiency of the *Abcg1* shRNA constructs was evaluated by Western blotting.

Western blotting

Western blotting was performed as previously reported (Lee da et al., 2010) using the primary antibodies listed in Table S4.

Intracranial injections

Injections were performed as previously described (Kaul et al., 2012). 2.5 to 3-week-old *Nf1*+/− and athymic (*nu/nu*) mice were used for these experiments. o-GSCs were implanted intracranially into the right side brainstem using a stereotactic device (coordinates = posterior 4.8 mm from the bregma, lateral 0.7 mm (right), and depth 4.5 from dura mater). Mice were euthanized 6 months later.

Immunostaining

Paraffin or frozen sections were processed (Dasgupta and Gutmann, 2005) prior to staining with appropriate antibodies (Table S4).

Microarray analysis

Mouse optic glioma neurospheres, *Nf1*−/− TVZ NSCs (TVZ_Cre) and wild-type TVZ NSCs (TVZ_LacZ) RNA was subjected to Affymetrix GeneChip Mouse Genome 430 2.0 Array hybridization, and the resulting data analyzed using Partex Genomics Suite Version 6.6 beta. These data have been deposited in the Gene Expression Omnibus (http://www.ncbi.nlm.nih.gov/geo/; accession number= GSE58260).

Real-time quantitative reverse transcription-PCR (qRT-PCR)

Real-time qRT-PCR was performed as previously described (Yeh et al., 2009) using the primers listed in Table S5. For each gene, the ΔΔCT values were calculated for each gene. *H3f3a* was used as an internal control.

Statistical analysis

Each experiment was performed with samples from at least three independent groups. Statistical significance was set at $P<0.05$ using the Student's *t*-test.

Supplementary Material

Refer to Web version on PubMed Central for supplementary material.

Acknowledgments

We thank Dr. Sara Taylor and Scott Gianino for technical assistance, Dr. Jason Weber for providing HeLa cells, and the Broad Institute RNAi Consortium (TRC), the Children's Discovery Institute (CDI), and The Genome Institute at Washington University (TGI). This work was funded by a grant from the Department of Defense (NF120032 to DHG). YHC is a recipient of the fellowship from the American Brain Tumor Association supported by the Emily Dorfman Foundation for Children in memory of Emily Ann Dorfman.

References

Bajenaru ML, Hernandez MR, Perry A, Zhu Y, Parada LF, Garbow JR, Gutmann DH. Optic nerve glioma in mice requires astrocyte Nf1 gene inactivation and Nf1 brain heterozygosity. Cancer Res. 2003; 63:8573–8577. [PubMed: 14695164]

Bao S, Wu Q, McLendon RE, Hao Y, Shi Q, Hjelmeland AB, Dewhirst MW, Bigner DD, Rich JN. Glioma stem cells promote radioresistance by preferential activation of the DNA damage response. Nature. 2006; 444:756–760. [PubMed: 17051156]

Beier D, Schulz JB, Beier CP. Chemoresistance of glioblastoma cancer stem cells--much more complex than expected. Mol Cancer. 2011; 10:128. [PubMed: 21988793]

Bleau AM, Hambardzumyan D, Ozawa T, Fomchenko EI, Huse JT, Brennan CW, Holland EC. PTEN/PI3K/Akt pathway regulates the side population phenotype and ABCG2 activity in glioma tumor stem-like cells. Cell Stem Cell. 2009; 4:226–235. [PubMed: 19265662]

Bonnet D, Dick JE. Human acute myeloid leukemia is organized as a hierarchy that originates from a primitive hematopoietic cell. Nat Med. 1997; 3:730–737. [PubMed: 9212098]

Booth L, Roberts JL, Cruickshanks N, Grant S, Poklepovic A, Dent P. Regulation of OSU-03012 Toxicity by ER Stress Proteins and ER Stress-Inducing Drugs. Mol Cancer Ther. 2014; 13:2384–2398. [PubMed: 25103559]

Carriere A, Cargnello M, Julien LA, Gao H, Bonneil E, Thibault P, Roux PP. Oncogenic MAPK signaling stimulates mTORC1 activity by promoting RSK-mediated raptor phosphorylation. Curr Biol. 2008; 18:1269–1277. [PubMed: 18722121]

Chen J, Li Y, Yu TS, McKay RM, Burns DK, Kernie SG, Parada LF. A restricted cell population propagates glioblastoma growth after chemotherapy. Nature. 2012; 488:522–526. [PubMed: 22854781]

Cho HY, Wang W, Jhaveri N, Lee DJ, Sharma N, Dubeau L, Schonthal AH, Hofman FM, Chen TC. NEO212, temozolomide conjugated to perillyl alcohol, is a novel drug for effective treatment of a broad range of temozolomide-resistant gliomas. Mol Cancer Ther. 2014; 13:2004–2017. [PubMed: 24994771]

Ciechomska IA, Gabrusiewicz K, Szczepankiewicz AA, Kaminska B. Endoplasmic reticulum stress triggers autophagy in malignant glioma cells undergoing cyclosporine a-induced cell death. Oncogene. 2013; 32:1518–1529. [PubMed: 22580614]

Daginakatte GC, Gutmann DH. Neurofibromatosis-1 (Nf1) heterozygous brain microglia elaborate paracrine factors that promote Nf1-deficient astrocyte and glioma growth. Hum Mol Genet. 2007; 16:1098–1112. [PubMed: 17400655]

Dasgupta B, Gutmann DH. Neurofibromin regulates neural stem cell proliferation, survival, and astroglial differentiation in vitro and in vivo. J Neurosci. 2005; 25:5584–5594. [PubMed: 15944386]

Erbay E, Babaev VR, Mayers JR, Makowski L, Charles KN, Snitow ME, Fazio S, Wiest MM, Watkins SM, Linton MF, et al. Reducing endoplasmic reticulum stress through a macrophage lipid chaperone alleviates atherosclerosis. Nat Med. 2009; 15:1383–1391. [PubMed: 19966778]

Galli R, Binda E, Orfanelli U, Cipelletti B, Gritti A, De Vitis S, Fiocco R, Foroni C, Dimeco F, Vescovi A. Isolation and characterization of tumorigenic, stem-like neural precursors from human glioblastoma. Cancer Res. 2004; 64:7011–7021. [PubMed: 15466194]

Golebiewska A, Bougnaud S, Stieber D, Brons NH, Vallar L, Hertel F, Klink B, Schrock E, Bjerkvig R, Niclou SP. Side population in human glioblastoma is non-tumorigenic and characterizes brain endothelial cells. Brain. 2013; 136:1462–1475. [PubMed: 23460667]

Guillamo JS, Creange A, Kalifa C, Grill J, Rodriguez D, Doz F, Barbarot S, Zerah M, Sanson M, Bastuji-Garin S, et al. Prognostic factors of CNS tumours in Neurofibromatosis 1 (NF1): a retrospective study of 104 patients. Brain. 2003; 126:152–160. [PubMed: 12477702]

Hale JS, Otvos B, Sinyuk M, Alvarado AG, Hitomi M, Stoltz K, Wu Q, Flavahan W, Levison B, Johansen ML, et al. Cancer stem cell-specific scavenger receptor 36 drives glioblastoma progression. Stem Cells. 2014; 32:1746–1758. [PubMed: 24737733]

Hegedus B, Banerjee D, Yeh TH, Rothermich S, Perry A, Rubin JB, Garbow JR, Gutmann DH. Preclinical cancer therapy in a mouse model of neurofibromatosis-1 optic glioma. Cancer Res. 2008; 68:1520–1528. [PubMed: 18316617]

Hegedus B, Hughes FW, Garbow JR, Gianino S, Banerjee D, Kim K, Ellisman MH, Brantley MA Jr, Gutmann DH. Optic nerve dysfunction in a mouse model of neurofibromatosis-1 optic glioma. J Neuropathol Exp Neurol. 2009; 68:542–551. [PubMed: 19525901]

Hope KJ, Jin L, Dick JE. Acute myeloid leukemia originates from a hierarchy of leukemic stem cell classes that differ in self-renewal capacity. Nat Immunol. 2004; 5:738–743. [PubMed: 15170211]

Horiguchi S, Takahashi J, Kishi Y, Morizane A, Okamoto Y, Koyanagi M, Tsuji M, Tashiro K, Honjo T, Fujii S, et al. Neural precursor cells derived from human embryonic brain retain regional specificity. J Neurosci Res. 2004; 75:817–824. [PubMed: 14994342]

Johnson GG, White MC, Wu JH, Vallejo M, Grimaldi M. The deadly connection between endoplasmic reticulum, Ca2+, protein synthesis, and the endoplasmic reticulum stress response in malignant glioma cells. Neuro Oncol. 2014; 16:1086–1099. [PubMed: 24569545]

Kaul A, Chen YH, Emnett RJ, Dahiya S, Gutmann DH. Pediatric glioma-associated KIAA1549:BRAF expression regulates neuroglial cell growth in a cell type-specific and mTOR-dependent manner. Genes Dev. 2012; 26:2561–2566. [PubMed: 23152448]

Kennedy MA, Barrera GC, Nakamura K, Baldan A, Tarr P, Fishbein MC, Frank J, Francone OL, Edwards PA. ABCG1 has a critical role in mediating cholesterol efflux to HDL and preventing cellular lipid accumulation. Cell Metab. 2005; 1:121–131. [PubMed: 16054053]

Kim CF, Jackson EL, Woolfenden AE, Lawrence S, Babar I, Vogel S, Crowley D, Bronson RT, Jacks T. Identification of bronchioalveolar stem cells in normal lung and lung cancer. Cell. 2005; 121:823–835. [PubMed: 15960971]

Kim HT, Kim IS, Lee IS, Lee JP, Snyder EY, Park KI. Human neurospheres derived from the fetal central nervous system are regionally and temporally specified but are not committed. Exp Neurol. 2006; 199:222–235. [PubMed: 16714017]

Kim KY, Ju WK, Hegedus B, Gutmann DH, Ellisman MH. Ultrastructural characterization of the optic pathway in a mouse model of neurofibromatosis-1 optic glioma. Neuroscience. 2010; 170:178–188. [PubMed: 20600672]

Klucken J, Buchler C, Orso E, Kaminski WE, Porsch-Ozcurumez M, Liebisch G, Kapinsky M, Diederich W, Drobnik W, Dean M, et al. ABCG1 (ABC8), the human homolog of the Drosophila white gene, is a regulator of macrophage cholesterol and phospholipid transport. Proc Natl Acad Sci U S A. 2000; 97:817–822. [PubMed: 10639163]

Kwiatkowski DJ, Zhang H, Bandura JL, Heiberger KM, Glogauer M, el-Hashemite N, Onda H. A mouse model of TSC1 reveals sex-dependent lethality from liver hemangiomas, and up-regulation of p70S6 kinase activity in Tsc1 null cells. Hum Mol Genet. 2002; 11:525–534. [PubMed: 11875047]

Lathia JD, Gallagher J, Heddleston JM, Wang J, Eyler CE, Macswords J, Wu Q, Vasanji A, McLendon RE, Hjelmeland AB, et al. Integrin alpha 6 regulates glioblastoma stem cells. Cell Stem Cell. 2010; 6:421–432. [PubMed: 20452317]

Lathia JD, Li M, Sinyuk M, Alvarado AG, Flavahan WA, Stoltz K, Rosager AM, Hale J, Hitomi M, Gallagher J, et al. High-throughput flow cytometry screening reveals a role for junctional adhesion molecule a as a cancer stem cell maintenance factor. Cell Rep. 2014; 6:117–129. [PubMed: 24373972]

Lee da Y, Gianino SM, Gutmann DH. Innate neural stem cell heterogeneity determines the patterning of glioma formation in children. Cancer Cell. 2012; 22:131–138. [PubMed: 22789544]

Lee da Y, Yeh TH, Emnett RJ, White CR, Gutmann DH. Neurofibromatosis-1 regulates neuroglial progenitor proliferation and glial differentiation in a brain region-specific manner. Genes Dev. 2010; 24:2317–2329. [PubMed: 20876733]

Li J, Lee AS. Stress induction of GRP78/BiP and its role in cancer. Curr Mol Med. 2006; 6:45–54. [PubMed: 16472112]

Lito P, Saborowski A, Yue J, Solomon M, Joseph E, Gadal S, Saborowski M, Kastenhuber E, Fellmann C, Ohara K, et al. Disruption of CRAF-mediated MEK activation is required for effective MEK inhibition in KRAS mutant tumors. Cancer Cell. 2014; 25:697–710. [PubMed: 24746704]

Liu G, Yuan X, Zeng Z, Tunici P, Ng H, Abdulkadir IR, Lu L, Irvin D, Black KL, Yu JS. Analysis of gene expression and chemoresistance of CD133+ cancer stem cells in glioblastoma. Mol Cancer. 2006; 5:67. [PubMed: 17140455]

Liu H, Bowes RC 3rd, van de Water B, Sillence C, Nagelkerke JF, Stevens JL. Endoplasmic reticulum chaperones GRP78 and calreticulin prevent oxidative stress, Ca2+ disturbances, and cell death in renal epithelial cells. J Biol Chem. 1997; 272:21751–21759. [PubMed: 9268304]

Liu WT, Huang CY, Lu IC, Gean PW. Inhibition of glioma growth by minocycline is mediated through endoplasmic reticulum stress-induced apoptosis and autophagic cell death. Neuro Oncol. 2013; 15:1127–1141. [PubMed: 23787763]

Louis DN, Ohgaki H, Wiestler OD, Cavenee WK, Burger PC, Jouvet A, Scheithauer BW, Kleihues P. The 2007 WHO classification of tumours of the central nervous system. Acta Neuropathol. 2007; 114:97–109. [PubMed: 17618441]

Luo B, Lee AS. The critical roles of endoplasmic reticulum chaperones and unfolded protein response in tumorigenesis and anticancer therapies. Oncogene. 2013; 32:805–818. [PubMed: 22508478]

Ma L, Chen Z, Erdjument-Bromage H, Tempst P, Pandolfi PP. Phosphorylation and functional inactivation of TSC2 by Erk implications for tuberous sclerosis and cancer pathogenesis. Cell. 2005; 121:179–193. [PubMed: 15851026]

Mahoney DH Jr, Cohen ME, Friedman HS, Kepner JL, Gemer L, Langston JW, James HE, Duffner PK, Kun LE. Carboplatin is effective therapy for young children with progressive optic pathway tumors: a Pediatric Oncology Group phase II study. Neuro Oncol. 2000; 2:213–220. [PubMed: 11265230]

Manning BD, Tee AR, Logsdon MN, Blenis J, Cantley LC. Identification of the tuberous sclerosis complex-2 tumor suppressor gene product tuberin as a target of the phosphoinositide 3-kinase/akt pathway. Mol Cell. 2002; 10:151–162. [PubMed: 12150915]

Nakata S, Campos B, Bageritz J, Bermejo JL, Becker N, Engel F, Acker T, Momma S, Herold-Mende C, Lichter P, et al. LGR5 is a marker of poor prognosis in glioblastoma and is required for survival of brain cancer stem-like cells. Brain Pathol. 2013; 23:60–72. [PubMed: 22805276]

Ozcan U, Yilmaz E, Ozcan L, Furuhashi M, Vaillancourt E, Smith RO, Gorgun CZ, Hotamisligil GS. Chemical chaperones reduce ER stress and restore glucose homeostasis in a mouse model of type 2 diabetes. Science. 2006; 313:1137–1140. [PubMed: 16931765]

Pace A, Vidiri A, Galie E, Carosi M, Telera S, Cianciulli AM, Canalini P, Giannarelli D, Jandolo B, Carapella CM. Temozolomide chemotherapy for progressive low-grade glioma: clinical benefits and radiological response. Ann Oncol. 2003; 14:1722–1726. [PubMed: 14630675]

Packer RJ, Ater J, Allen J, Phillips P, Geyer R, Nicholson HS, Jakacki R, Kurczynski E, Needle M, Finlay J, et al. Carboplatin and vincristine chemotherapy for children with newly diagnosed progressive low-grade gliomas. J Neurosurg. 1997; 86:747–754. [PubMed: 9126887]

Packer RJ, Lange B, Ater J, Nicholson HS, Allen J, Walker R, Prados M, Jakacki R, Reaman G, Needles MN, et al. Carboplatin and vincristine for recurrent and newly diagnosed low-grade gliomas of childhood. J Clin Oncol. 1993; 11:850–856. [PubMed: 8487049]

Parry PV, Engh JA. Knockdown of LGR5 suppresses the proliferation of glioma cells in vitro and in vivo. Neurosurgery. 2014; 74:N14–15. [PubMed: 24435145]

Pietras A, Katz AM, Ekstrom EJ, Wee B, Halliday JJ, Pitter KL, Werbeck JL, Amankulor NM, Huse JT, Holland EC. Osteopontin-CD44 signaling in the glioma perivascular niche enhances cancer stem cell phenotypes and promotes aggressive tumor growth. Cell Stem Cell. 2014; 14:357–369. [PubMed: 24607407]

Pong WW, Higer SB, Gianino SM, Emnett RJ, Gutmann DH. Reduced microglial CX3CR1 expression delays neurofibromatosis-1 glioma formation. Ann Neurol. 2013; 73:303–308. [PubMed: 23424002]

Raabe EH, Lim KS, Kim JM, Meeker A, Mao XG, Nikkhah G, Maciaczyk J, Kahlert U, Jain D, Bar E, et al. BRAF activation induces transformation and then senescence in human neural stem cells: a pilocytic astrocytoma model. Clin Cancer Res. 2011; 17:3590–3599. [PubMed: 21636552]

Ricci-Vitiani L, Lombardi DG, Pilozzi E, Biffoni M, Todaro M, Peschle C, De Maria R. Identification and expansion of human colon-cancer-initiating cells. Nature. 2007; 445:111–115. [PubMed: 17122771]

Sakariassen PO, Immervoll H, Chekenya M. Cancer stem cells as mediators of treatment resistance in brain tumors: status and controversies. Neoplasia. 2007; 9:882–892. [PubMed: 18030356]

See WL, Tan IL, Mukherjee J, Nicolaides T, Pieper RO. Sensitivity of glioblastomas to clinically available MEK inhibitors is defined by neurofibromin 1 deficiency. Cancer Res. 2012; 72:3350–3359. [PubMed: 22573716]

Singh SK, Clarke ID, Terasaki M, Bonn VE, Hawkins C, Squire J, Dirks PB. Identification of a cancer stem cell in human brain tumors. Cancer Res. 2003; 63:5821–5828. [PubMed: 14522905]

Singh SK, Hawkins C, Clarke ID, Squire JA, Bayani J, Hide T, Henkelman RM, Cusimano MD, Dirks PB. Identification of human brain tumour initiating cells. Nature. 2004; 432:396–401. [PubMed: 15549107]

Son MJ, Woolard K, Nam DH, Lee J, Fine HA. SSEA-1 is an enrichment marker for tumor-initiating cells in human glioblastoma. Cell Stem Cell. 2009; 4:440–452. [PubMed: 19427293]

Suzuki K, Gerelchuluun A, Hong Z, Sun L, Zenkoh J, Moritake T, Tsuboi K. Celecoxib enhances radiosensitivity of hypoxic glioblastoma cells through endoplasmic reticulum stress. Neuro Oncol. 2013; 15:1186–1199. [PubMed: 23658321]

Tarling EJ, Bojanic DD, Tangirala RK, Wang X, Lovgren-Sandblom A, Lusis AJ, Bjorkhem I, Edwards PA. Impaired development of atherosclerosis in Abcg1−/− Apoe−/− mice: identification of specific oxysterols that both accumulate in Abcg1−/− Apoe−/− tissues and induce apoptosis. Arterioscler Thromb Vasc Biol. 2010; 30:1174–1180. [PubMed: 20299684]

Tarling EJ, Edwards PA. ATP binding cassette transporter G1 (ABCG1) is an intracellular sterol transporter. Proc Natl Acad Sci U S A. 2011; 108:19719–19724. [PubMed: 22095132]

Taylor MD, Poppleton H, Fuller C, Su X, Liu Y, Jensen P, Magdaleno S, Dalton J, Calabrese C, Board J, et al. Radial glia cells are candidate stem cells of ependymoma. Cancer Cell. 2005; 8:323–335. [PubMed: 16226707]

Tchoghandjian A, Baeza N, Colin C, Cayre M, Metellus P, Beclin C, Ouafik L, Figarella-Branger D. A2B5 cells from human glioblastoma have cancer stem cell properties. Brain Pathol. 2010; 20:211–221. [PubMed: 19243384]

Tchoghandjian A, Fernandez C, Colin C, El Ayachi I, Voutsinos-Porche B, Fina F, Scavarda D, Piercecchi-Marti MD, Intagliata D, Ouafik L, et al. Pilocytic astrocytoma of the optic pathway: a tumour deriving from radial glia cells with a specific gene signature. Brain. 2009; 132:1523–1535. [PubMed: 19336457]

Vermeulen L, Todaro M, de Sousa Mello F, Sprick MR, Kemper K, Perez Alea M, Richel DJ, Stassi G, Medema JP. Single-cell cloning of colon cancer stem cells reveals a multi-lineage differentiation capacity. Proc Natl Acad Sci U S A. 2008; 105:13427–13432. [PubMed: 18765800]

Wang D, Zhou J, Fan C, Jiao F, Liu B, Sun P, Miao J, Zhang Q. Knockdown of LGR5 suppresses the proliferation of glioma cells in vitro and in vivo. Oncol Rep. 2014; 31:41–49. [PubMed: 24172981]

Wang N, Lan D, Chen W, Matsuura F, Tall AR. ATP-binding cassette transporters G1 and G4 mediate cellular cholesterol efflux to high-density lipoproteins. In Proc Natl Acad Sci U S A. 2004:9774–9779.

Wojcik AJ, Skaflen MD, Srinivasan S, Hedrick CC. A critical role for ABCG1 in macrophage inflammation and lung homeostasis. J Immunol. 2008; 180:4273–4282. [PubMed: 18322240]

Xue J, Wei J, Dong X, Zhu C, Li Y, Song A, Liu Z. ABCG1 deficiency promotes endothelial apoptosis by endoplasmic reticulum stress-dependent pathway. J Physiol Sci. 2013; 63:435–444. [PubMed: 23897420]

Yeh TH, Lee da Y, Gianino SM, Gutmann DH. Microarray analyses reveal regional astrocyte heterogeneity with implications for neurofibromatosis type 1 (NF1)-regulated glial proliferation. Glia. 2009; 57:1239–1249. [PubMed: 19191334]

Yvan-Charvet L, Pagler TA, Seimon TA, Thorp E, Welch CL, Witztum JL, Tabas I, Tall AR. ABCA1 and ABCG1 protect against oxidative stress-induced macrophage apoptosis during efferocytosis. Circ Res. 2010; 106:1861–1869. [PubMed: 20431058]

Yvan-Charvet L, Ranalletta M, Wang N, Han S, Terasaka N, Li R, Welch C, Tall AR. Combined deficiency of ABCA1 and ABCG1 promotes foam cell accumulation and accelerates atherosclerosis in mice. J Clin Invest. 2007; 117:3900–3908. [PubMed: 17992262]

Zinszner H, Kuroda M, Wang X, Batchvarova N, Lightfoot RT, Remotti H, Stevens JL, Ron D. CHOP is implicated in programmed cell death in response to impaired function of the endoplasmic reticulum. Genes Dev. 1998; 12:982–995. [PubMed: 9531536]

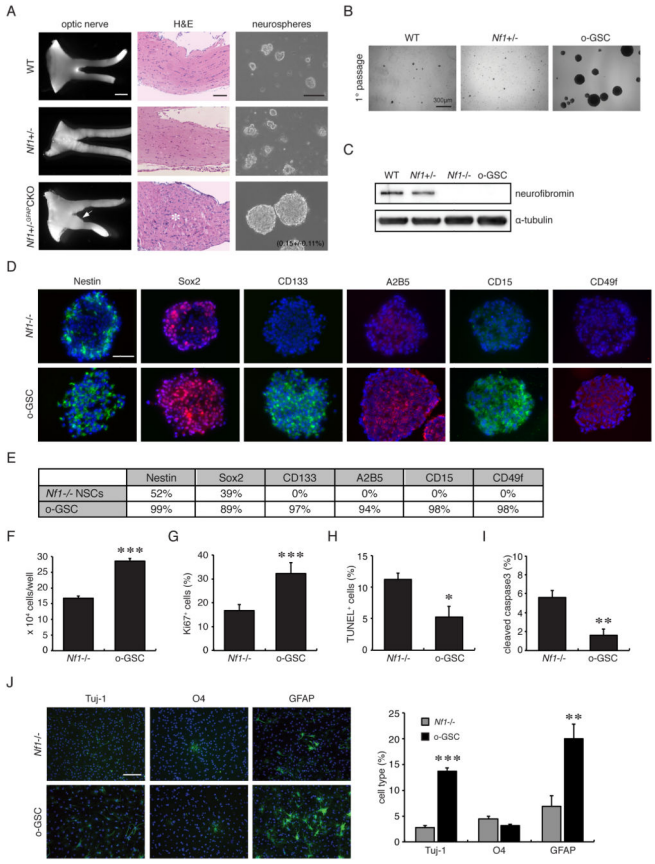

Figure 1. Neurospheres can only be generated from 3-month-old optic glioma-bearing mice

(**A**) Optic gliomas from 3-month-old *Nf1*+/−^{GFAP}CKO mice have increased optic nerve volumes (white arrow) and abnormal cell clusters (white asterisk) within the optic nerves and chiasm. Neurospheres were only observed in cultures from 3-month-old *Nf1*+/−^{GFAP}CKO mice, but not from wild-type (WT), *Nf1*$^{flox/flox}$, or *Nf1*+/− mice. (**B**) After the initial passage, secondary neurospheres formed only in the o-GSC cultures. Scale bar, 300 μm. (**C**) Loss of neurofibromin expression was observed in o-GSCs and *Nf1*−/− TVZ NSCs. (**D**) Similar to *Nf1*−/− TVZ NSCs, neurospheres from optic gliomas express Nestin and Sox2. CD133, A2B5, CD15 and CD49f expression were only observed in o-GSCs. (**E**) Quantitation of cell type-specific markers. In addition, o-GSCs (passage 8–10) have increased (**F**) cell numbers and (**G**) percentages of Ki67^{+} cells, but (**H, I**) decreased cell apoptosis compared to *Nf1*−/− TVZ NSCs. (**J**) Increased glial differentiation was observed in o-GSCs relative to *Nf1*−/− TVZ NSCs (passage 8). Nuclei were counterstained with DAPI. Values denote the mean ± SD. Scale bars: optic nerve, 1000 μm; H&E 100 μm; o-GSCs 100 μm. (*) p<0.05; (**) p<0.01; (***) p<0.001.

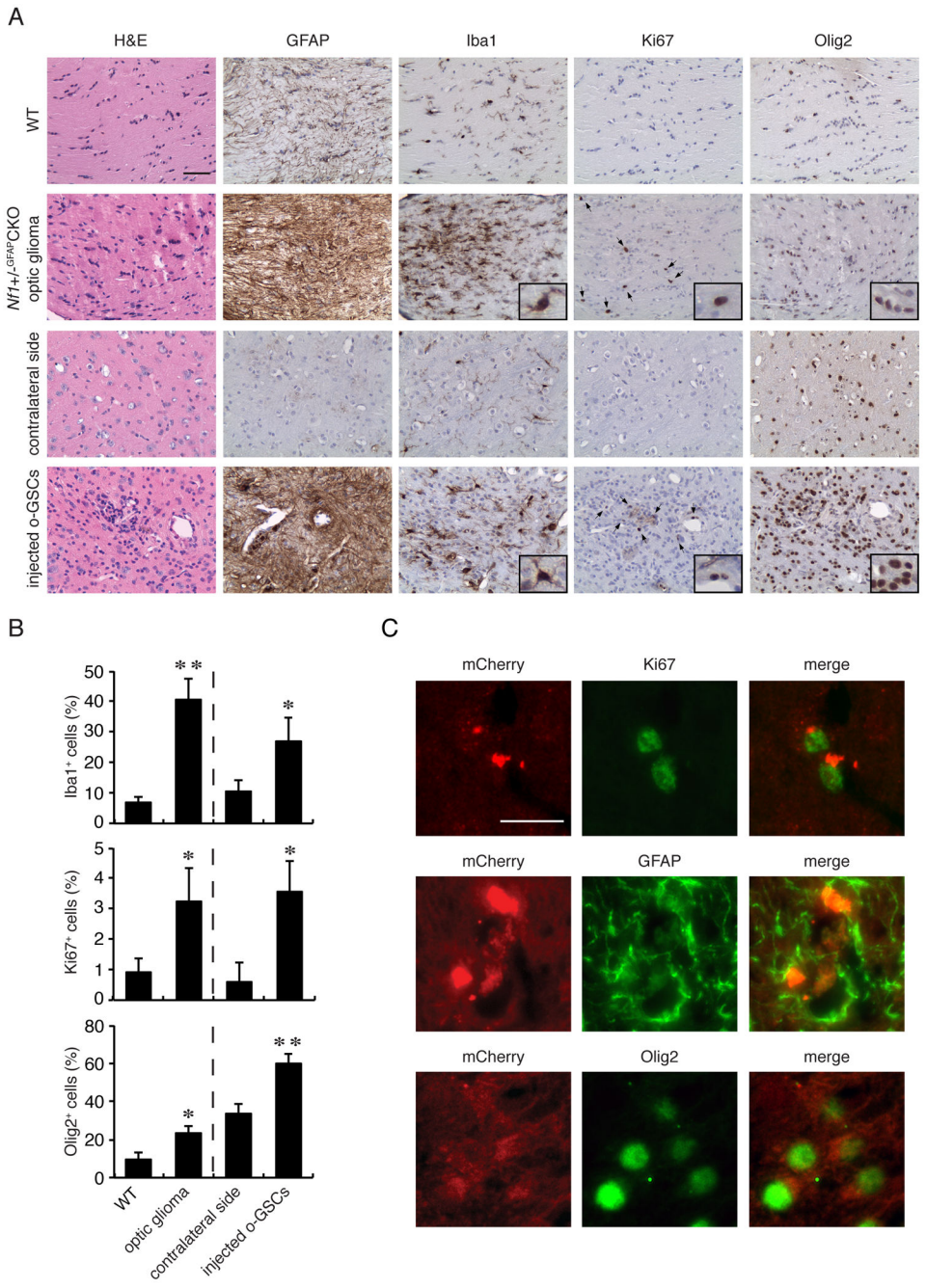

Figure 2. o-GSCs form glioma-like lesions following injection into *Nf1*+/− mice, similar to the parent tumors

(**A, B**) Abnormal cell clusters, hypercellularity (H&E), increased number of glial fibrillary acidic protein (GFAP)-immunoreactive cells, increased Iba1$^+$ cells (inset), increased Ki67$^+$ cells (arrows and inset; A), and increased Olig2$^+$ cells (inset) were observed in both the parent optic glioma tumors and ectopic o-GSC lesions (n=4 per group). Wild-type optic nerves or the contralateral uninjected sides were used as reference controls. (**C**) Immunofluorescence co-labeling shows transgene (mCherry) expression in Ki67-, GFAP-

and Olig2-immunoreactive cells at the injection site. Error bars denote mean ± SD. Scale bars: IHC 50 μm; IF 10 μm. (*) $p<0.05$; (**) $p<0.01$.

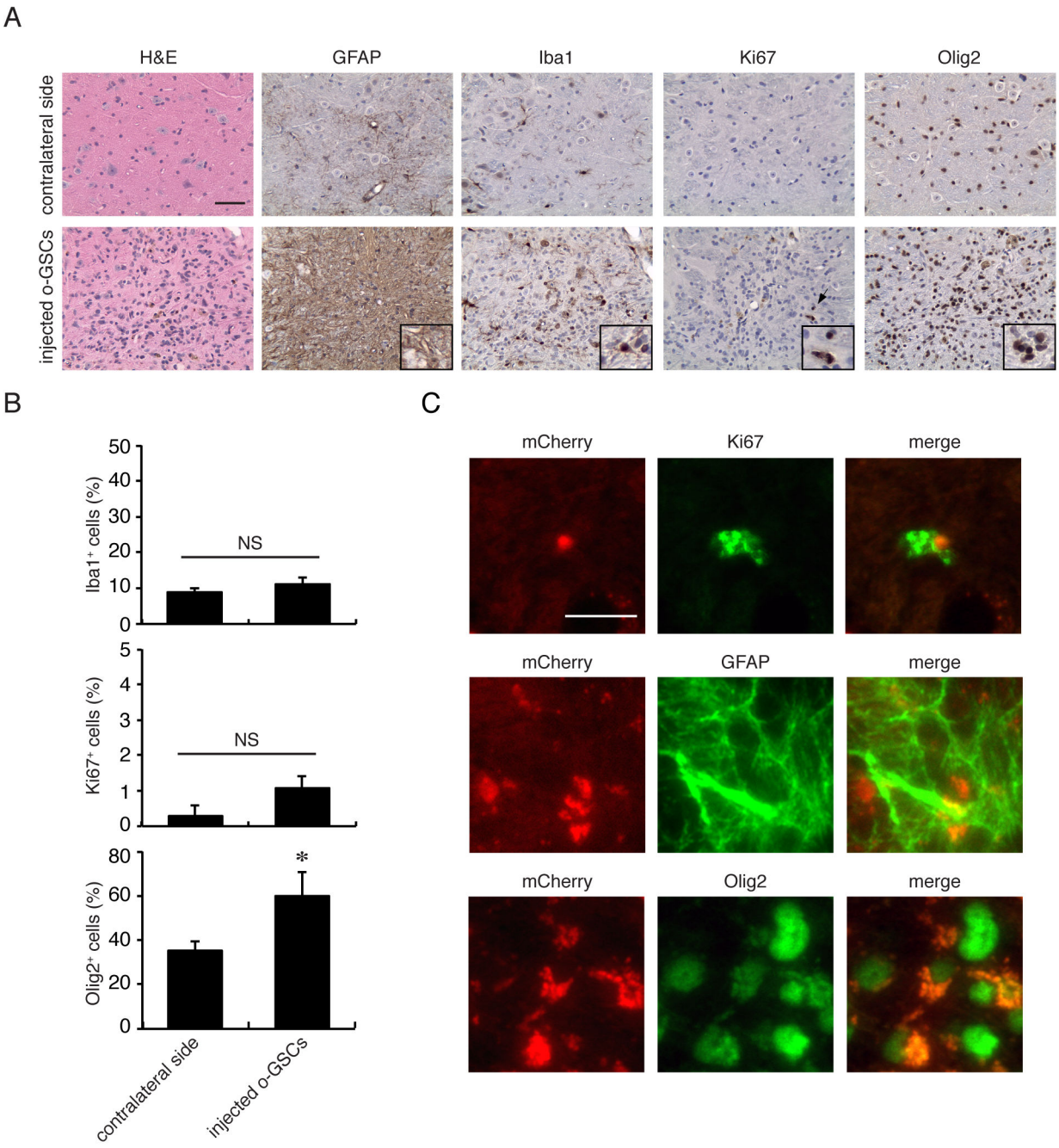

Figure 3. o-GSCs do not form similar glioma-like lesions following injection into athymic mice

(**A**) Only three of the five athymic mice injected with o-GSC showed increased cellularity (H&E) and increased numbers of GFAP-immunoreactive cells. While increased Iba1$^+$ cells (inset), Ki67$^+$ cells (arrows and inset; A), and Olig2$^+$ cells (inset) were observed at the injection sites relative to contralateral sides, (**B**) the percentages of Iba1$^+$ and Ki67$^+$ cells found at the o-GSC injection sites were similar to those on the contralateral (uninjected) sides. (**C**) Immunofluorescence co-labeling reveals mCherry expression in Ki67-, GFAP-

and Olig2-immunoreactive cells at the injection site. Error bars denote mean ± SD. Scale bars: IHC 50 μm; IF 10 μm. NS, not significant. (*) $p<0.05$.

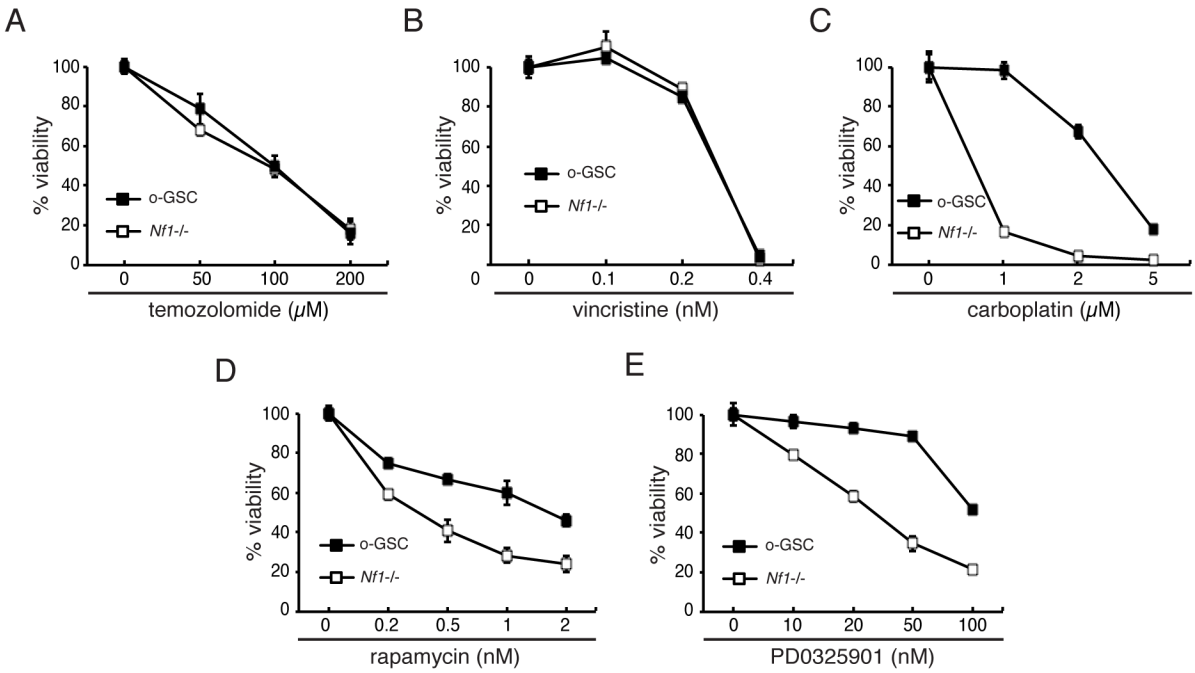

Figure 4. o-GSCs exhibit relative resistance to carboplatin, rapamycin and PD0325901, but not to temozolomide and vincristine, treatments

(**A, B**) Both stem cell populations show similar dose responses to temozolomide and vincristine. (**C**) o-GSCs exhibit relative resistance to carboplatin, (**D**) rapamycin and (**E**) PD0325901 (PD901) treatment compared to *Nf1*-deficient TVZ NSCs. Error bars denote mean ± SD.

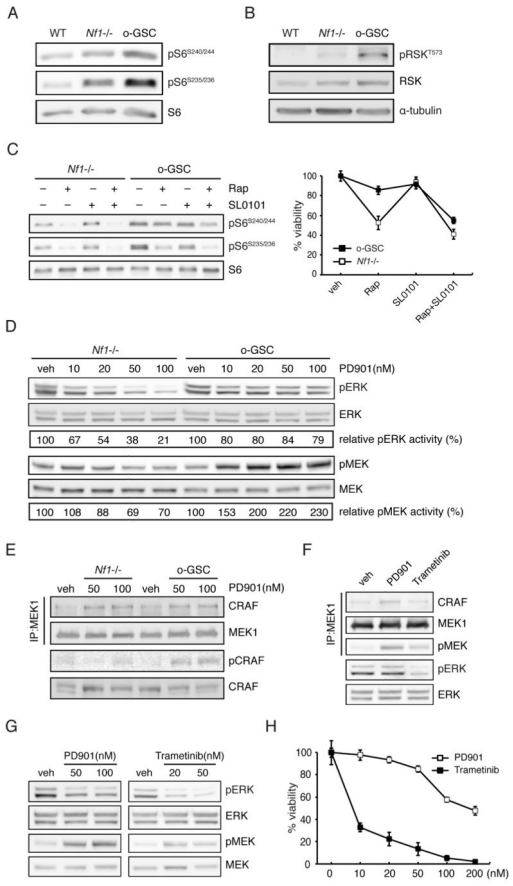

Figure 5. Mechanisms underlying the relative resistance of o-GSCs to rapamycin and PD0325901 treatments

Increased (**A**) mTOR activation (S6 phosphorylation) and (**B**) p90-RSK Thr^{573} phosphorylation were observed in o-GSCs relative to *Nf1*−/− TVZ NSCs. (**C**) *Nf1*-deficient TVZ NSCs and o-GSCs were treated with rapamycin (0.5nM) and SL0101 (50μM) as indicated. S6 phosphorylation and the percentage of viable cell number are shown. (**D**) PD901 treatment did not inhibit ERK phosphorylation due to aberrant MEK activation (phosphorylation) in o-GSCs. (**E**) PD901 treatment induces the formation of MEK1-CRAF complexes, but increased CRAF phosphorylation was only observed in o-GSCs. Trametinib (50nM) reduced (**F**) CRAF/MEK binding, (**G**) MEK/ERK phosphorylation and (**H**) o-GSC growth.

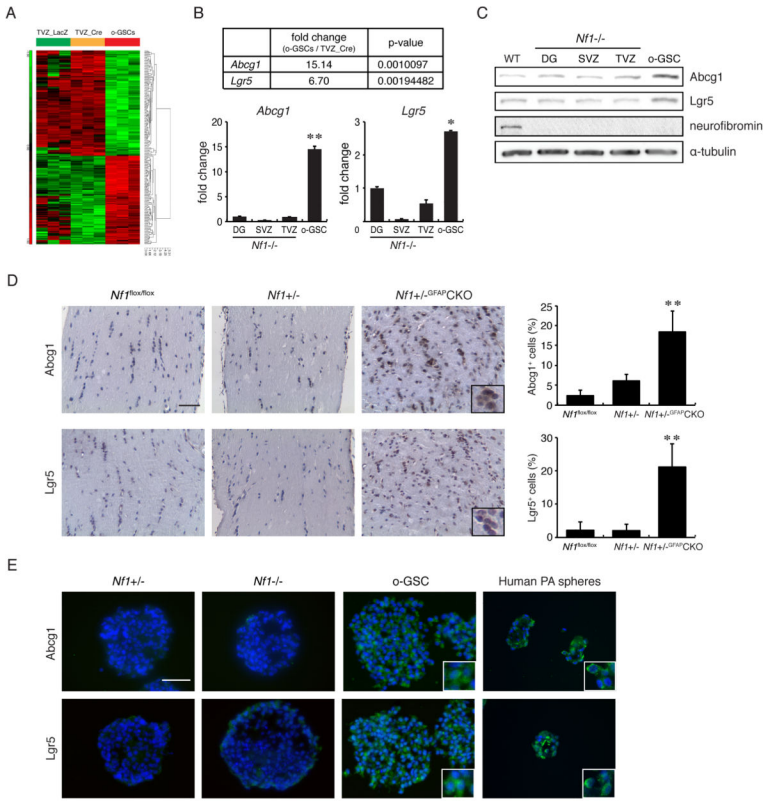

Figure 6. o-GSCs exhibit increased Abcg1 expression

(**A**) Hierarchical cluster analysis of WT (TVZ_LacZ), *Nf1*−/− (TVZ_Cre) NSCs, and o-GSCs. Three independent arrays representing each sample are shown. The expression level represents standardized values from −5 (green, <1-fold change) to 5 (red, >1-fold change). No change is denoted by black. Differential expression of two candidate genes, *Abcg1* and *Lgr5*, was validated by (**B**) qPCR and (**C**) Western blotting. (**D**) Increased numbers of Abcg1^{+} and Lgr5^{+} cells were found in *Nf1* mouse optic gliomas compared to non-tumor-bearing optic nerve sections from WT (*Nf1*$^{flox/flox}$) and *Nf1*+/− mice (n=4 per group). (**E**) Immunocytochemistry reveals Lgr5 and Abcg1 expression in mouse o-GSCs and spheres from human PAs. DG, dentate gyrus; SVZ, subventricular zone; TVZ, third ventricle. Error bars denote mean ± SD. Nuclei are counterstained with DAPI. Scale bars, 100 μm. (*) $p<0.01$; (**) $p<0.001$.

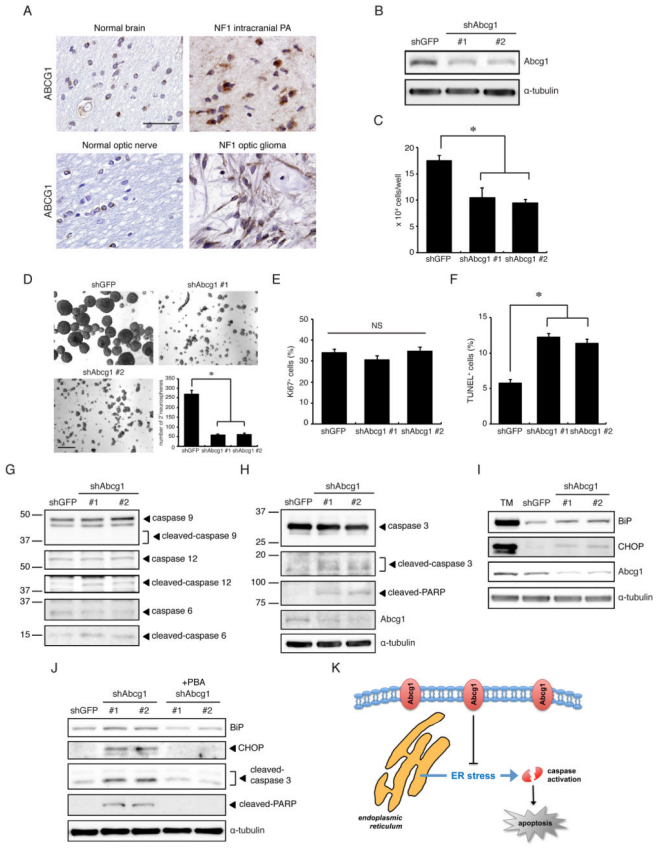

Figure 7. Abcg1 expression maintains o-GSC growth

(**A**) Glioma specimens from six individuals with NF1 exhibit ABCG1 expression relative to age-matched control brains. Scale bar, 50 μm. (**B**) shRNA knockdown of o-GSC Abcg1 expression. shAbcg1 knockdown reduced (**C**) o-GSC growth and (**D**) decreased self-renewal. Scale bar, 200 μm. Following Abcg1 knockdown, there was (**E**) no change in proliferation (% $Ki67^+$ cells); however, and (**F**) increased apoptosis (% $TUNEL^+$ cells) were observed. (**G, H**) Abcg1 knockdown induced caspase-3, caspase-6, caspase-12, and PARP, but not caspase-9, cleavage. (**I**) Increased BiP and CHOP expression was observed following Abcg1 knockdown. Tunicamycin (TM) (2μg/ml) was included as a control to induce ER stress. (**J**) Expression of BiP, CHOP, cleaved-caspase-3 and cleaved-PARP was decreased following Abcg1 knockdown in o-GSCs treated with PBA (2mM), an ER stress inhibitor. (**K**) Proposed mechanism underlying Abcg1 maintenance of o-GSC survival through suppression of ER stress. Error bars denote mean ± SD. NS, not significant. (*) $p<0.01$.